

# Collinear investigation of laser initiated reduced density channels

L. D. Horton and R. M. Gilgenbach

Nuclear Engineering Department, The University of Michigan, Ann Arbor Michigan 48109

(Received 30 August 1983; accepted for publication 22 September 1983)

The characteristics of reduced density channels generated by laser initiated discharges have been investigated by means of collinear holographic interferometry and schlieren photography. We report the first direct measurements of the density profiles in the interior of such channels. Under unperturbed conditions these channels exhibit azimuthal asymmetries. Gas dynamics within the channel are also presented for the case of incident shock waves reflected from cylindrical and planar boundaries.

PACS numbers: 52.50.Jm, 52.70. — m, 52.25.Lp

One promising technique for light ion and electron beam transport through gas blankets in inertial confinement fusion (ICF) reactors employs reduced density channels generated by laser guided discharges (LGD).<sup>1-6</sup> Recently, such discharges have also been demonstrated to provide a new technique for rapid melting and hole boring in materials.<sup>7</sup> These channels also provide a reproducible means of lightning simulation.

In this letter we report the first direct measurement of density profiles in the interior of channels by means of collinear holographic interferometry and collinear schlieren photography. In these collinear diagnostics, the ruby laser probe beam is directed parallel to and on axis with the channel. This differs from other experiments<sup>6,8,9</sup> which have employed transverse schlieren and interferometry diagnostics. Transverse diagnostics require Abel inversion to deduce the radial density profile.<sup>6,9</sup> Our new collinear diagnostic configurations have also made it possible to study azimuthal symmetry and effects occurring in the interior of channels from passing shock waves. Hydrodynamic simulations by Picone *et al.*<sup>10,11</sup> at the Naval Research Labs (NRL) have shown that the azimuthal symmetry of such channels is crucial in determining the growth time for turbulent convective mixing.

A brief description of the experimental configuration is given here; Ref. 3 provides more details. A high intensity pulse (0.10 GW) from a transverse, excited, atmospheric CO<sub>2</sub> laser is focused by a 2.5-m focal length gold mirror. High voltage discharge electrodes are located across the length of CO<sub>2</sub> laser induced breakdown plasma. These electrodes consist of thin pointed rods, which minimize electrode effects on the ends of the channel. A capacitor (0.04  $\mu$ F) charged to 30 kV is discharged through the channel 5  $\mu$ s after the laser pulse. Typical peak discharge channel currents are 10 kA. The uniformity and decay time of channels generated by this experiment have been demonstrated<sup>3</sup> to closely resemble the longer channels at NRL.<sup>8</sup>

The collinear ruby laser diagnostics exploit the hollow center of the annular CO<sub>2</sub> laser beam. Two turning mirrors are placed in this open center away from the focal point. This directs the ruby laser probe beam on axis with the CO<sub>2</sub> laser and discharge. Collinear interferometry and schlieren photography have been performed on separate discharges. The holographic interferometry system uses the double exposure method to obtain horizontal reference fringes. Schlieren

photography is performed using a circular aperture to give two-dimensional spatial resolution.<sup>8</sup> Since the ruby laser pulse width (20 ns full width at half-maximum) is short compared to channel hydrodynamic time scales, these ruby laser diagnostics give a "snapshot" of the channel density evolution.

Radial density profiles obtained from collinear holo-

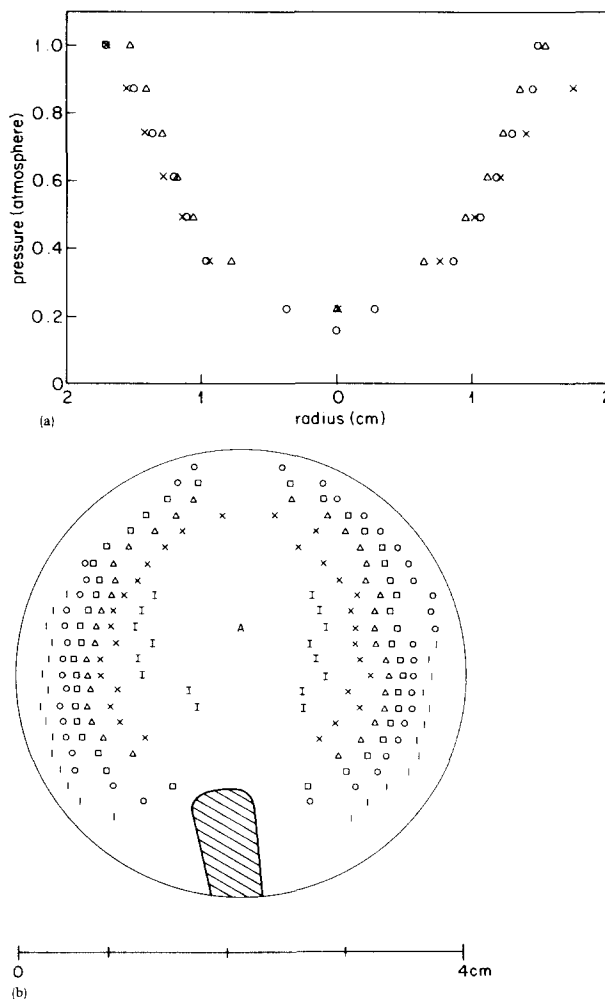


FIG. 1. Data obtained by collinear holographic interferometry for 6-cm laser guided discharge channels in helium. (a) Radial density profile through center of channel at times: (O) = 31  $\mu$ s, ( $\Delta$ ) = 51  $\mu$ s, (X) = 71  $\mu$ s. (b) Density contours at 71  $\mu$ s: (|) = 1 atm, (O) = 0.87 atm, ( $\square$ ) = 0.74 atm, ( $\Delta$ ) = 0.61 atm, (X) = 0.49 atm, (I) = 0.36 atm, (A) = 0.22 atm.

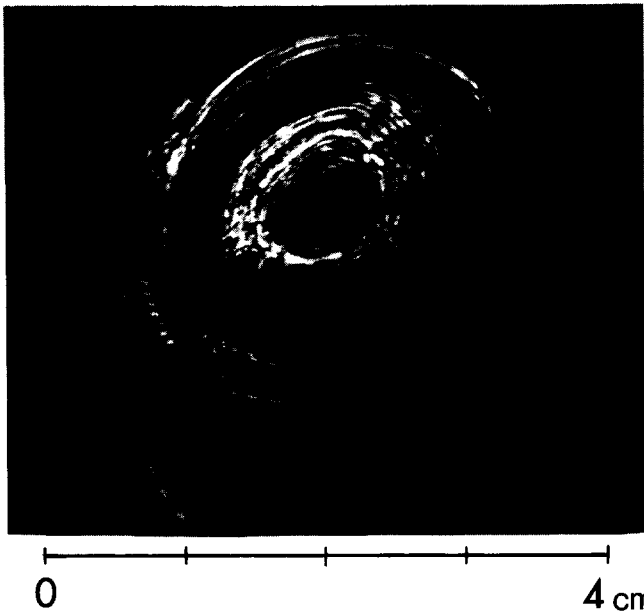


FIG. 2. Collinear holographic interferogram of a laser guided discharge channel in argon taken  $71 \mu\text{s}$  after discharge.

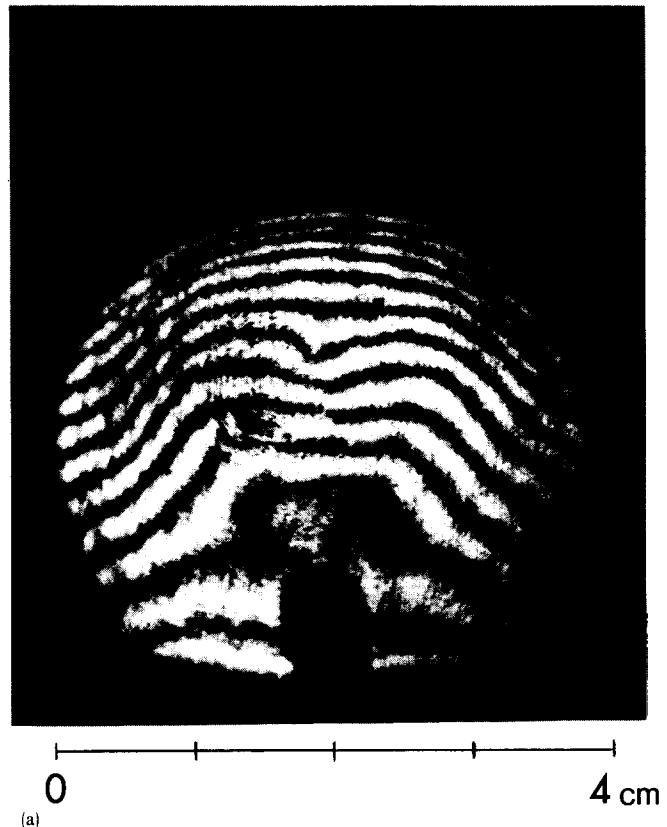
graphic interferometry (CHI) of laser guided discharge channels in helium are given in Fig. 1(a). These data show that the gas density decreases from atmospheric at the edge to 0.22 atm at the center. These helium channels exhibited slight azimuthal asymmetries, as shown in the density contours of Fig. 1(b).

More obvious interferometric data concerning channel ellipticity have been obtained for gases with a higher index of refraction than helium. For argon and air the index of refraction was large enough to produce fringes which encircled the channel axis. A holographic interferogram for a LGD in argon is shown in Fig. 2. Analysis of a number of such interferograms has shown that these laser guided discharge channels exhibit ellipticities up to 1.6. This ellipticity could be due to nonuniform ohmic heating by the discharge or initial asymmetries in the laser induced breakdown.

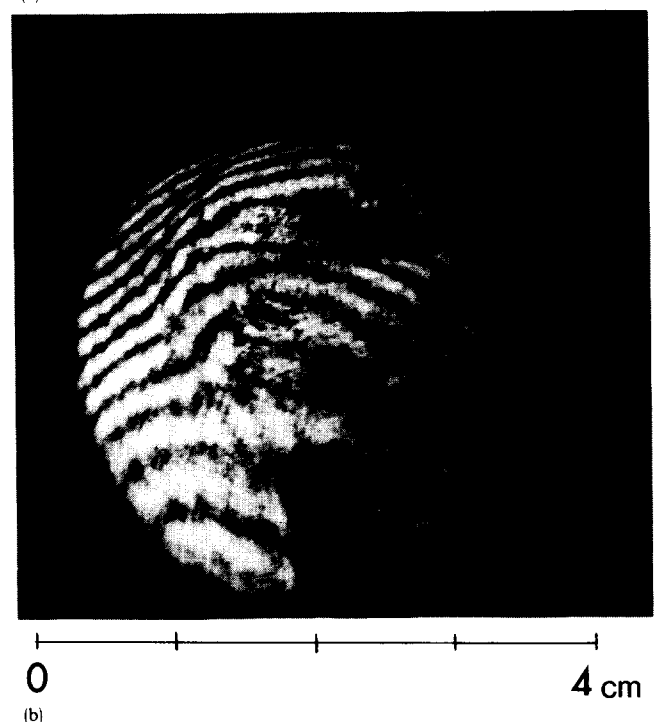
Figure 3 gives collinear holographic interferograms for the cases of an unperturbed (helium) channel and for a channel through which a shock wave has propagated. The shock wave had a velocity of about 1600 m/s after reflection from a planar boundary. Three effects are apparent in the CHI of Fig. 3(b). First, the channel axis has been shifted in the same direction as the passing shock wave. Second, the channel density profile has become asymmetric, exhibiting a steeper density gradient on the side on which the shock emerged. Third, turbulent mixing has begun within the channel interior after passage of the shock. Note that all three of these effects have been predicted in hydrodynamic simulations by Picone *et al.*<sup>11</sup>

An additional interesting feature can be seen in the unperturbed interferogram of Fig. 3(a). Several of our interferograms, including this one, have shown a slight density increase at the channel center. This is the first observation of this effect, which is not understood at this time.

Collinear schlieren data for  $\text{CO}_2$  laser induced air breakdown channels are presented in Fig. 4. At early times, the data clearly show a concentric series of expanding shock



(a)



(b)

FIG. 3. Collinear holographic interferograms of LGD in helium ( $51 \mu\text{s}$  after discharge): (a) unperturbed case and (b) with shock wave reflected from planar boundary located 2 cm to the right of channel axis.

waves from the chain of  $\text{CO}_2$  laser induced breakdown beads. These shock waves have been shown to coalesce into a single cylindrical shock.<sup>8</sup> Asymmetries which appear at times up to  $20 \mu\text{s}$  are related to the focal intensity distribution of the  $\text{CO}_2$  laser, as seen from burn patterns on thermal sensitive paper. When a cylindrical boundary is placed around the laser induced breakdown channel (center column

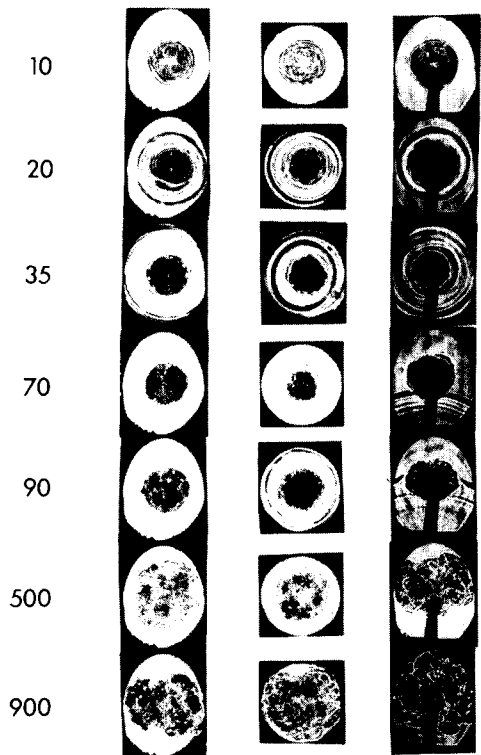


FIG. 4. Collinear schlieren photos of CO<sub>2</sub> laser induced breakdown channels in air. Left-hand column is unbounded case, center column has 3.2 cm i.d. cylindrical boundary, and right-hand column has planar boundary 1.6 cm below channel axis. Times listed to the left are in  $\mu$ s.

in Fig. 4), the gas flow behind the shock wave appears to cause a compression of the channel diameter at 70  $\mu$ s. Data for the single planar boundary (right column of Fig. 4) clear-

ly illustrate that normal shock reflection is occurring; in this case the gas flow from the shock appears to pull the channel away from the boundary at 500  $\mu$ s.

Turbulent convective mixing of hot channel gas embedded in cold gas is related to the vorticity ( $\xi$ ) by <sup>10</sup>

$$\frac{d\xi}{dt} + \xi \nabla \cdot \mathbf{v} = \xi \cdot \nabla \mathbf{v} + \frac{[\nabla \rho \times \nabla P]}{\rho^2} \quad (1)$$

Here,  $P$  is the pressure,  $\rho$  is the density, and  $v$  is the fluid velocity. The final term of Eq. (1) provides a mechanism for shocks to rapidly increase the vorticity, by the cross product of the shock's pressure jump with density gradients. This could explain the rapid turbulent mixing observed in the presence of reflected shocks.

We acknowledge valuable discussions with Dr. J. R. Greig. This research was supported by ONR Project NR-012-756 and NSF grant ECS-8105966.

<sup>1</sup>J. R. Greig, D. W. Koopman, R. F. Fernsler, R. E. Pechacek, I. M. Vitkovitsky, and A. W. Ali, *Phys. Rev. Lett.* **41**, 174 (1978).

<sup>2</sup>D. W. Koopman and K. A. Saum, *J. Appl. Phys.* **44**, 5328 (1973).

<sup>3</sup>L. D. Horton and R. M. Gilgenbach, *Phys. Fluids* **25**, 1702 (1982).

<sup>4</sup>G. Yonas, *Sci. Amer.* **239**, 50 (1978).

<sup>5</sup>P. A. Miller, R. I. Butler, M. Cowan, J. R. Freeman, J. W. Poukey, T. P. Wright, and G. Yonas, *Phys. Rev. Lett.* **39**, 92 (1977).

<sup>6</sup>J. N. Olsen and L. Baker, *J. Appl. Phys.* **52**, 3286 (1982).

<sup>7</sup>R. M. Gilgenbach, O. E. Ulrich, and L. D. Horton, *Rev. Sci. Instrum.* **54**, 109 (1983).

<sup>8</sup>M. Raleigh, J. R. Greig, R. E. Pechacek, and E. Laikin, *NRL Memorandum Report No. 4380*, February 13, 1981.

<sup>9</sup>M. Raleigh and J. R. Greig, *NRL Memorandum Report 4390*, Feb. 12, 1981.

<sup>10</sup>J. M. Picone and J. P. Boris, *Phys. Fluids* **26**, 365 (1983).

<sup>11</sup>J. M. Picone, E. S. Oram, J. P. Boris, and T. R. Young, submitted to *Proceedings of the 9th Int. Colloq. on the Dynamics of Explosions and Reactive Systems*, Poitiers, France, July 3-8, 1983 (unpublished).

## Electron kinetics of silane discharges

A. Garscadden, G. L. Duke, and W. F. Bailey

*Air Force Wright Aeronautical Laboratories and Air Force Institute of Technology, Wright-Patterson AFB, Ohio 45433*

(Received 27 May 1983; accepted for publication 16 September 1983)

A numerical solution of the Boltzmann transport equation for electrons has been used to calculate the electron energy distribution function in silane for a range of applied steady-state fields. This enables the evaluation of the fractional energy transfer for vibrational excitation and dissociation, the rate coefficients for the different processes and the electron transport properties.

PACS numbers: 51.10.+y, 51.50.+v, 34.50.Ez, 82.30.Lp

The plasma decomposition of silane in various gas mixtures is important in the preparation of hydrogenated amorphous silicon thin films.<sup>1</sup> Experimental measurements<sup>2,3</sup> have shown that the film properties are sensitive to the plasma excitation conditions. Therefore, it is of considerable interest to define the actual electron kinetics of silane discharges. Recent measurements of several excitation and ionization cross sections<sup>4-6</sup> have permitted our calculation of the actual electron energy distribution function for silane plasmas. Then moments of the distribution function were calculated and yield the electron transport properties and electron kinetics of silane gas mixtures of plasma deposition reactor interest.

A numerical solution<sup>7</sup> of the Boltzmann transport equation was employed, along with the latest experimental electron impact cross sections to obtain the electron energy distribution for various gas mixtures as a function of  $E/N$ , where  $E$  is the applied electric field in V/cm and  $N$  is the total gas density. These distribution functions were then integrated to obtain the electron drift velocity, mean energy, and electron impact excitation rates. The set of cross sections used for silane consisted of momentum transfer,<sup>8</sup> vibrational excitation,<sup>8</sup> ionization,<sup>4</sup> and dissociative excitation.<sup>5</sup> To complete the cross-section set, a total electron dissociation cross section was assumed to be linear with a threshold at the photodissociation threshold of 7.8 eV, and reaching a value